Transformation of Contrails into Cirrus during SUCCESS

Patrick Minnis, David F. Young, and Donald P. Garber
NASA Langley Research Center, Hampton, Virginia

Louis Nguyen, William L. Smith, Jr., and Rabindra Palikonda
Analytical Services and Materials, Inc., Hampton, Virginia

Geophysical Research Letters SUCCESS Special Issue
Accepted November 1997

Transformation of Contrails into Cirrus during SUCCESS

Patrick Minnis, David F. Young, and Donald P. Garber
NASA Langley Research Center, Hampton, Virginia

Louis Nguyen, William L. Smith, Jr., and Rabindra Palikonda
Analytical Services and Materials, Inc., Hampton, Virginia

Abstract. Three contrail systems were analyzed with geostationary satellite data to document the conversion of the contrails to cirrus clouds. Two unique contrails, a pair of figure eights and a NASA DC-8 oval, were tracked for more than 7 hours. A cluster of contrails from commercial aircraft lasted over 17 hours. The figure eights produced a cirrus cloud having a maximum extent of 12,000 km^2; the commercial cluster reached an area of ~35,000 km^2. The contrail-cirrus were thin with optical depths between 0.2 and 0.5. In all cases, cloud particle size increased as the contrails developed into cirrus clouds. The climatic impact of contrails will be greater than would be estimated if only linear contrails, those typically observed in satellite imagery, are considered. Additional research is required to obtain reliable statistics on contrail growth and lifetime.

Introduction

Contrails, as anthropogenic cirrus clouds, affect both the radiation and hydrological cycle in a manner similar to other cirrus clouds except that they may have different microphysical properties [e.g., *Gayet et al*., 1996]. In many cases, these clouds would not exist but for the aircraft exhaust. They are also distinct in their narrow, linear shapes. As commercial air traffic has increased, contrails have become a more common feature in the skies of industrialized countries. In the contiguous U. S., contrails are observed, on average, ~10% of the time when the upper troposphere is unobscured by low clouds [*Minnis et al.*, 1997]. Because of their small areal extent, contrails as identified by their usual linear appearance, are unlikely to have a significant impact on climate. Any casual observer of the skies has probably observed the occasional spreading and growth of contrails. Such observations suggest that contrails may often be more than just short-lived linear clouds. If large areas of persistent cirrus are produced from contrails, then aircraft-induced clouds may have a more significant effect on the climate than is currently believed.

Because of strong winds in the upper troposphere, it is difficult to discern the complete lifetime of a contrail-induced cloud from the Sun-synchronous satellites typically used to study contrails. To learn more about the lifetimes of contrails, this paper uses data from the Geostationary Operational Environmental Satellite (GOES) and NOAA Advanced Very High Resolution Radiometer (AVHRR) to detect, track, and analyze several contrail systems during NASA's Subsonic Clouds and Contrails Effects Special Study (SUCCESS) conducted in spring 1996.

Data and Methodology

In general, satellite detection of contrails over southern Kansas and northern Oklahoma was difficult during SUCCESS because they were either infrequent or occurred simultaneously with cirrus. This study focuses on 3 days during SUCCESS when particular contrails were easily distinguishable from nearby cirrus clouds. A figure-eight contrail system is tracked over the Gulf of Mexico during April 11, 1996 using 1-km multispectral data from NOAA-14 AVHRR and half-hourly, 4-km data from the GOES-8 imager channels with wavelengths: 0.65-μm (visible, VIS), 3.9-μm (solar infrared, SI), 11-μm (infrared, IR), and 12-μm (split window, SW). Data from GOES-8 at 75°W, NOAA-12, and NOAA-14 are used to observe several commercial aircraft contrail systems over Oklahoma, Kansas, and Texas during April 16. An oval-shaped contrail produced by the NASA DC-8 on the afternoon of May 12 off the Oregon coast is followed with GOES-9 at 135°W and NOAA-12 AVHRR.

A contrail is detected either as a distinct linear or other geometrical cold feature in the IR imagery or by using the difference, *BTD*, between the IR and SW brightness temperatures, T_{IR} and T_{SW}, respectively. Once identified, a box is drawn around the contrail and all pixels having $T_{IR} < T_T$, (where T_T is an IR threshold temperature) and $BTD \geq 2$K are assumed to be part of the contrail cloud. The areal coverage C of the contrail pixels is determined as the product of the area per pixel and the number of contrail-cloud pixels. The contrail VIS optical depth τ, effective diameter D of the cloud ice particles, and temperature T_c are derived from the multispectral data using two approaches described by *Minnis et al*. [1995] and the layer bispectral threshold method (LBTM; *Minnis et al.*, [1993]). The VIS-IR-SI technique (VIST) is used for solar zenith angles less than 78°, while the SI-IR-SW technique (SIST) can be applied at all hours. The VIST can provide reliable values of τ and D for a greater range of optical depths and mixture of cloud heights. The SIST can be used at all hours but works best for single-layer cloud systems. Because it is based on emitted radiation, the SIST can only retrieve τ and D for optically thin clouds. *Young et al*. [1997] showed that the VIST can accurately retrieve D for relatively homogeneous wave clouds, while the SIST produces relatively accurate values of T_c and reasonable values of τ and D for cirrus clouds at night [*Smith et al*., 1997]. The LBTM uses only VIS and IR data to derive T_c and τ assuming D = 41 μm. Details of the VIST analysis for SUCCESS are given by *Young et al*. [1997].

Results and Discussion

April 11, 1996

A figure eight is evident off the Texas coast in enhanced 1-km IR (Figure 1a) and VIS (Figure 1b) imagery from NOAA-14 at 1915 UTC. Part of another contrail-like feature forms a sideways "V" to the east of the eight. The figure eight is nearly invisible in the VIS image which reveals an abundance of bright low-level clouds. As the eight feature moves eastward, it grows and becomes clearly discernible in the 2045 UTC GOES-8 IR image (Figure 1c) which shows both the "V" feature (outside of the box) and a second, nearly complete figure eight to the west. The double figure eight was tracked as it moved to the east across the Gulf of Mexico south of Louisiana (Figure 1d) until it disappeared at ~0345 UTC, April 12 (Figure 1e). The figure

eights' original lengths and widths together exceeded 90 and 80 km, respectively. This feature moved at an average speed of 36 ms^{-1} which corresponds to an altitude between 9.0 and 10.8 km and a temperature between 243 and 233 K based on soundings from Lake Charles, LA at 1200 UTC, April 11 and 0000 UTC, April 12. The origin of this feature and its initial formation time are unknown. Clearly, it is an aircraft-derived cloud.

The VIST and SIST results for the double figure eight are summarized in Figure 2. For the first 3 hours after 1900 UTC, T_c (Figure 2a) is between 250 and 260 K. The SIST indicates that T_c decreases to approximately 225 K by 0200 UTC before increasing again as the contrail disappears. At 1915 UTC, the area covered by the figure eight (Figure 2b) is ~6000 km^2 and gradually increases to 12,300 km^2 by 0100 UTC when it begins a rapid dissipation. Both analyses indicate that D is initially small (20 - 30 μm) and grows steadily. The SIST analysis retrieves a maximum particle size of 90 μm by 2245 UTC that decreases again after 0000 UTC. The cloud optical depth (Figure 2c) from both techniques is ~0.30 for the first 3 hours followed by a decrease to 0.1 when the areal coverage peaks.

The cirrus cloud produced by the figure eight probably began earlier than 1915 UTC over southern Texas or northern Mexico. Some of the analyses, especially in the early hours are likely to be contaminated by the low clouds seen in the imagery. Few low clouds are evident in the imagery east of the eight at 1912 UTC. Cloud temperatures determined from the analyses were generally warmer, by at least 10K, than the apparent temperature of the cloud based on the soundings. This overestimate of temperature may be due to several factors. The optical depth of the cloud is extremely small and, therefore, subject to large uncertainty. The correction for semitransparency is sensitive to uncertainties in both τ and clear-sky temperature T_{cs}. For example, the minimum IR brightness temperature observed within the contrail at 2045 UTC is 283 K compared to T_{cs} = 291 K. For most of the pixels, T_c is closer to 288 K. Slight errors in τ for these small temperature differences will have a significant effect on the value of T_c. Partially filled pixels will also cause similar problems. Another source of the problem may be that the actual relationship between the VIS and IR optical depths for these clouds differs from the theoretical one used here because of differences between the assumed and actual particle shapes.

Some of the temperature discrepancy may be due to the formation of larger particles that precipitate taking much of the mass into lower levels. Since the IR is more sensitive to the larger particles, the effect would be an observation weighted to the lowest level. In this instance, T_c = 250 K would correspond to an altitude of ~7.2 km suggesting a vertical extent of more than 2 km, a reasonable value for cirrus clouds. This mechanism may also explain the spreading of the contrail. As the particles fall into lower levels, they travel at slower speeds tilting the cloud so that its horizontal dimension increases with time. When the moisture for precipitation becomes depleted, the mean particle size will decrease and only the top portion of the cloud will remain before completely dissipating. The growth of particle size corresponds to an increase in area that ends shortly after D, τ and T_c drop dramatically. The final dissipation phase repeats the process. Such a scenario for this case is plausible if the trends in the results are accurate.

April 16, 1996

A cluster of contrails, apparently from commercial aircraft, formed over southeastern New Mexico between 1300 and 1400 UTC. These contrails are evident at 1515 UTC in the GOES-8 imagery (Figure 3a) showing a fan-shaped region with linear features that is separate from, but ahead, of a mass of advancing frontal cirrus. These contrails either formed and produced some thin cirrus or formed in and thickened existing thin cirrus clouds. At 1945 UTC (Figure 3b), the cluster of contrails moved over north central Texas. Another set of fanning contrails is evident in the lower left corner of Figure 3b. The subject cluster advected eastward over Louisiana (Figure 3c) and Alabama (Figure 3d) before it passed out of the available GOES image area over Georgia at 0645 UTC, April 17. Throughout the life of this system, it remained isolated from any other cloud mass and was the only cloud seen over much of the southeast during the night. A NOAA-14 AVHRR IR close-up of the cluster in Figure 3e reveals the fan shape and linear features. A VIST analysis of D

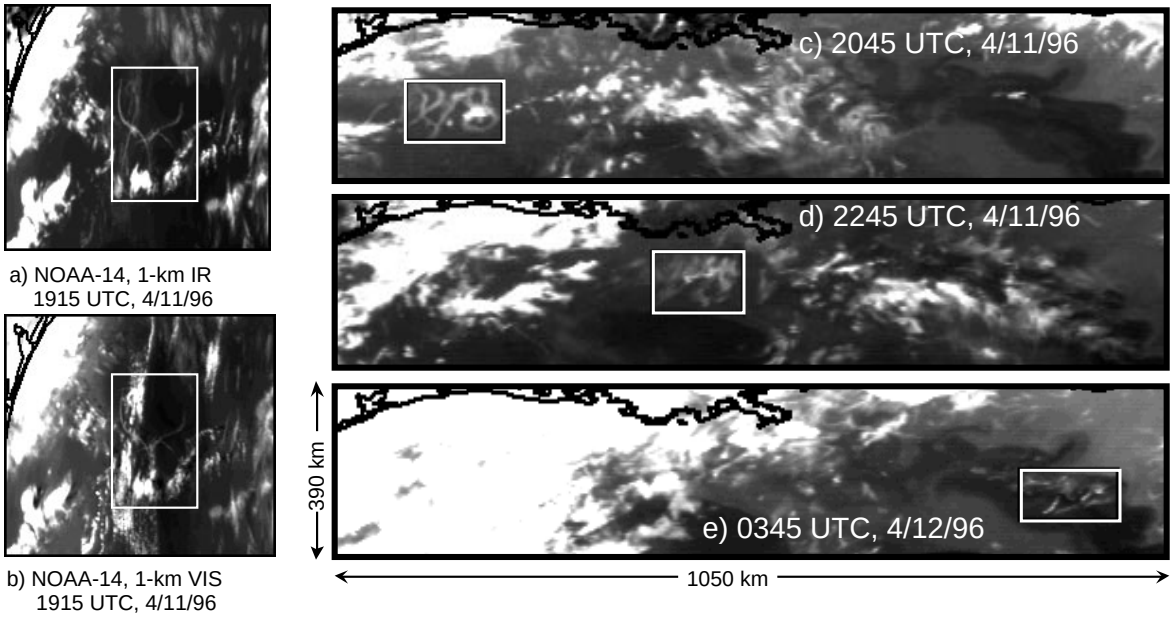

Figure 1. Figure eight contrails and cirrus development from (a-b) NOAA-14 IR and VIS and (c-e) GOES-8 IR imagery.

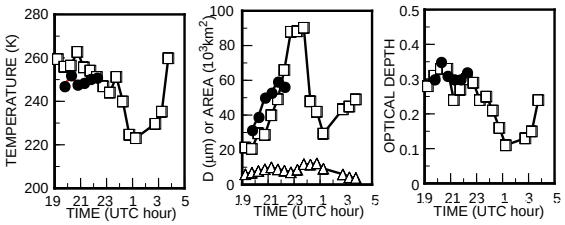

Figure 2. Cloud parameters from figure-eight contrails over Gulf of Mexico for 11-12 April 1996. Closed symbols from VIST analysis. Open symbols from SIST. Triangles refer to area.

in the inset box shows the small particles characteristic of contrails with *D* between 12 and 25 μm for most of the distinct linear features. Some of the contrails are indicated with the numbered arrows. No-retrieval areas (in gray), where no solution could be obtained in the analysis, generally correspond to very thin clouds which produce ambiguous changes in the clear-sky (black areas) radiances.

The contrail area at 1515 UTC was ~11,500 km^2. The cirrus cover increased rapidly to ~35,000 km^2 by 1700 UTC, then remained relatively constant at ~23,000 km^2 from 1800 UTC to 0200 UTC, April 17 (Figure 3f). The contrail area was only analyzed through 0345 UTC, April 17 when it was 17,100 km^2. It appeared to slowly diminish in size as it continued through Georgia. Cloud temperature from VIST (Figure 3g) varies between 250 and 260 K as in the figure-eight case. T_c from the SIST starts at ~240K and slowly increases to ~250 K. The LBTM cloud temperatures, ranging from 220 to 245 K, are probably more realistic than the others because they correspond to altitudes between 8 and 10.5 km that are typical of commercial flight routes. The primary differences between the LBTM and VIST temperatures arise because the LBTM uses all of the pixels to estimate a mean temperature. The VIST uses only the brightest pixels, which often contain cloud sides, resulting in a smaller correction for semitransparency (note the slightly larger optical depths from the VIST in Figure 3h). It leaves out many of the "dark" cirrus pixels which are cold and optically thin and have a darker-than-normal background because of shadows cast by thicker clouds nearby [see *Minnis et al.*, 1993]. The VIS reflectance of these pixels is less than or equal to the mean clear-sky reflectance. In many cases, half of the pixels were in this shadowed or dim category and could not be used in the VIST. The SIST temperatures are less subject to the shadowing but are more sensitive to the T_{cs} which varies due to clear shadows and the high frequency of cold lakes evident in Figure 3e.

Optical depths range between 0.2 and 0.8, with lower values returned consistently by the SIST. During daytime, the LBTM and VIST results are probably more reliable because of the sensitivity of the VIS reflectance to τ. The increase in τ coincides with the areal development of the cloud. Cloud particle size (Figure 3i) derived from the VIST increases steadily from 19 μm at 1515 UTC to 60 μm at 2245 UTC. The SIST retrieval yields larger crystals that increase up to 70 μm after 2245 UTC. The VIST retrievals for the high-resolution data in Figure 3e are consistent with the GOES-8 results at 1945 UTC. Overall, the VIST results reinforce the notion that small-particle contrails develop into cirrus with typically larger particle sizes.

May 12, 1996

The NASA DC-8 flew a racetrack pattern (Figure 4a) at 10 km several times off the California coast near 2200 UTC, May 12, 1996. This flight produced a contrail that was barely detectable in the GOES-9 imagery by 2315 UTC (Figure 4b). The contrail grew rapidly as it advected across the coast and over the Sacramento Valley (Figures 4c-e). At 0245 UTC, May 13, its leading edge reached the Sierra Nevada. A close-up of the 1-km 12-μm image from NOAA-12 (Figure 4f) shows that the oval has almost filled in completely with streaks oriented northwest to southeast. The contrail continued filling (Figure 4h) until it broke up over the Sierra Nevada by 0545 UTC (Figure 4i).

Analysis of this contrail was complicated by the variable background of low clouds over the Pacific, coastal contrasts, warm valleys, and cold mountains. The SIST analysis in Figure 5 shows the cloud temperature initially at 257 K dropping to 232 K by 2345 UTC and back up to ~245 K for several hours before decreasing again over the mountains. The temperature at 10 km in the San Francisco sounding at 0000 UTC was ~230 K. The first temperature value is probably inaccurate because of the small signal from the contrail (Figure 4b) while the next observation is probably more reliable. The LBTM was used to determine τ and T_c at 2345 UTC for the portion of the contrail over a clear patch of water by the coast. Its cloud temperature agrees with the SIST retrieval (Figure 5a), but τ is smaller (Figure 5c) by 0.1. Another LBTM analysis, performed when the entire

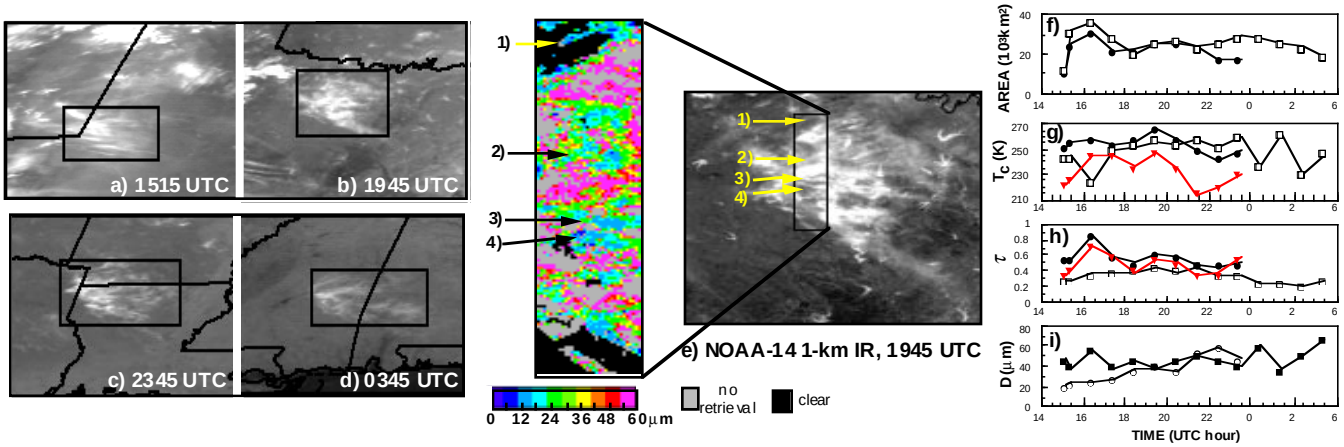

Figure 3. Contrail cluster changing into cirrus clouds April 16-17, 1996 beginning over southeastern New Mexico. (a-d) GOES-8 IR imagery, (e) D from AVHRR data, (f-i) VIST (solid circles), SIST (open squares), and LBTM (triangles) results from GOES-8.

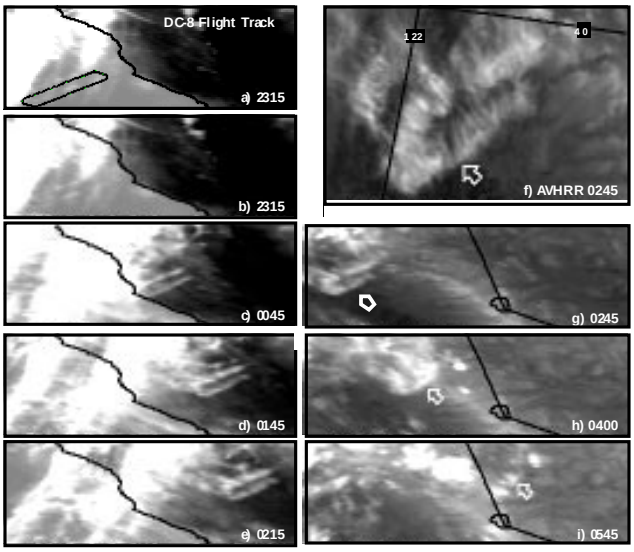

Figure 4. Development of racetrack contrail as observed by NOAA-12 SW (f) and GOES-8 IR imagery (a-e and g-i).

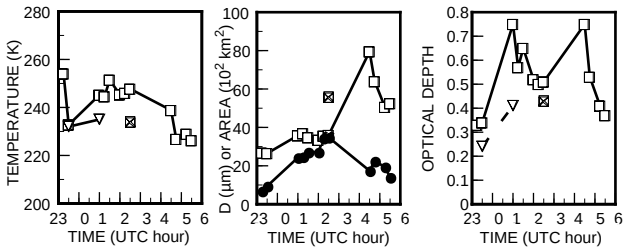

Figure 5. Cloud parameters computed for racetrack contrail from GOES-9 and NOAA-12 data taken May 12-13, 1996. Single points refer to NOAA-12 results. Solid symbols: contrail area in (b). Triangles: LBTM results. Temperature: contrail temperature.

contrail had crossed the coast at 0045 UTC, yielded T_c = 234 K and τ = 0.4 compared to 242 K and 0.55 from the SIST retrieval. The SIST was also applied to the NOAA-12 data and produced T_c = 234 K and τ = 0.42 at 0245 UTC, values that are also less than the GOES-8 counterparts. Both the LBTM and NOAA-12 SIST analyses have the benefit of more accurate values of T_{cs} compared to the GOES-8 SIST because of the extra channels and better resolution. The range of results is probably indicative of the retrieval accuracies. From all of the data, it is clear that the contrail cloud grows steadily to a maximum coverage of ~3500 km^2 at 0245 UTC before breaking up. The cloud optical depth increases to between 0.4 and 0.8, while the particle size increases from ~27 μm to 35 μm at 0145 UTC, then increases to 80 μm before the cloud dissipates.

Concluding Remarks

Three contrail systems have been examined here that lasted from a minimum of 7 to over 17 hours. The optical depths, on average, ranged from 0.2 to 0.5 over the cloud lifetime. In all cases, cloud particle sizes grew from small, contrail-sized values to larger crystal sizes typical of natural cirrus. A single plane, in the case of the figure eight, produced a cirrus cloud covering over 12,000 km^2. The one commercial cluster examined here grew to over 35,000 km^2. All three cases studied here show that contrails can develop into cirrus fields that would probably be unrecognizable as contrails to a surface observer. Furthermore, without the benefit of geostationary satellites, these systems would be mistaken by satellite observers as natural cirrus for much of their lifetimes. It may be concluded from these limited results that aircraft exhaust can produce cirrus clouds that cover much more area than the simple linear features commonly observed in satellite data. These findings suggest that a considerable amount of ice-supersaturated air exists that does not produce clouds because of the absence of nucleating mechanisms. The aircraft exhaust provides the trigger for producing these clouds that probably would not develop otherwise.

How often contrails convert to extensive cirrus, how long they maintain themselves, and how much area they cover are still open, difficult questions. Contrails often form in the vicinity of cirrus or may cause cloud formation earlier than would otherwise happen. Separating the effects of cirrus-contrail coverage and lifetime is not a trivial problem. Given the frequent occurrence of contrails and the results shown here, it is clear that contrails have the potential for a significant climatic effect, at least on a regional scale. The cases used here were selected because they were well-defined systems. Growing contrails were evident over significant portions of the imagery outside of the subject clouds and could have been chosen to make the point. Determination of the climatic effects of contrails will require much additional study using both observational and modeling techniques to help separate natural and anthropogenic effects.

Acknowledgments. This research was supported by the NASA Subsonic Assessment Program and First ISCCP Regional Experiment Program through NASA/Office of Mission to Planet Earth. The manuscript was typeset by Joanne H. Saunders of Analytical Services and Materials, Inc.

References

Gayet. J.-F., G. Febvre, G, Brogniez, H. Chepfer, W. Renger, and P. Wendling, Microphysical and optical properties of cirrus and contrails: Cloud field study on 13 October 1989. *J. Atmos. Sci.*, 53, 126-138, 1996.

Minnis, P., J. K. Ayers, and S. P. Weaver, Contrail frequency of occurrence over the U.S. from surface observations during 1993-1994, NASA RP 1404, in press, 1997.

Minnis, P., P. W. Heck, and D. F. Young, Inference of cirrus cloud properties from satellite-observed visible and infrared radiances. Part II: Verification of theoretical radiative properties. *J. Atmos. Sci.*, 50, 1305-1322, 1993.

Minnis, P., D. P. Kratz, J. A. Coakley, Jr., M. D. King, R. Arduini, D. P. Garber, P. W. Heck, S. Mayor, W. L. Smith, Jr., and D. F. Young, Cloud optical property retrieval (Subsystem 4.3). "Clouds and the Earth's Radiant Energy System (CERES) Algorithm Theoretical Basis Document, Volume III: Cloud Analyses and Radiance Inversions (Subsystem 4)," *NASA RP 1376 Vol. 3*, edited by CERES Science Team, pp. 135-176, December, 1995.

Smith, W. L., Jr., L. Nguyen, D. P. Garber, D. F. Young, P. Minnis, and J. Spinhirne, Comparisons of cloud heights derived from satellite and ARM surface lidar data. *Proc. 6th ARM Science Team Meeting*, San Antonio, TX, March 4-7, 1996, 287-291, 1997.

Young, D. F., P. Minnis, D. Baumgardner and H. Gerber, Comparisons of effective particle sizes in wave clouds during SUCCESS. *Geophys. Res. Ltrs.*, this issue, 1997.

D. P. Garber, P. Minnis, and D. F. Young, NASA Langley Research Center, Hampton, Virginia.

L. Nguyen, R. Palikonda, and W. L. Smith, Jr., Analytical Services and Materials, Inc., Hampton, Virginia.

Received July 7, 1997; revised October 29, 1997;
accepted October 31, 1997

(*Geophysical Research Letters* SUCCESS Special Issue October 1997.)